

Long-range angular correlations by strong color fields in hadronic collisions

Kevin Dusling

Physics Department, North Carolina State University, Raleigh, NC 27695, USA

I present an overview of the *ridge* phenomenon in proton-proton and proton-lead collisions. This novel collimation between rapidity separated hadron pairs is a consequence of non-linear gluon dynamics within the small- x wave-function of the colliding hadrons.

Multi-particle correlations in high-energy hadronic collisions can serve as sensitive tests of QCD dynamics. In the fall of 2010 the CMS collaboration made a striking discovery¹. In high-multiplicity proton-proton collisions a correlation was uncovered between charged-particle pairs having a large pseudo-rapidity separation ($\Delta\eta \gg 1$) and a narrow angular separation ($\Delta\phi \lesssim 1$) in azimuth. Figure 1 displays the original CMS result. As the structure of the two-particle correlation resembles a mountain range the new discovery was dubbed “The Ridge” when it was first observed in heavy-ion collisions. It should be stressed that the heavy-ion ridge has a unique physical interpretation from the ridge in p+p and p+Pb collisions. While the former is attributed primarily to final-state rescattering and hydrodynamic flow the latter, which will be the focus of this proceeding, is a consequence of gluon saturation².

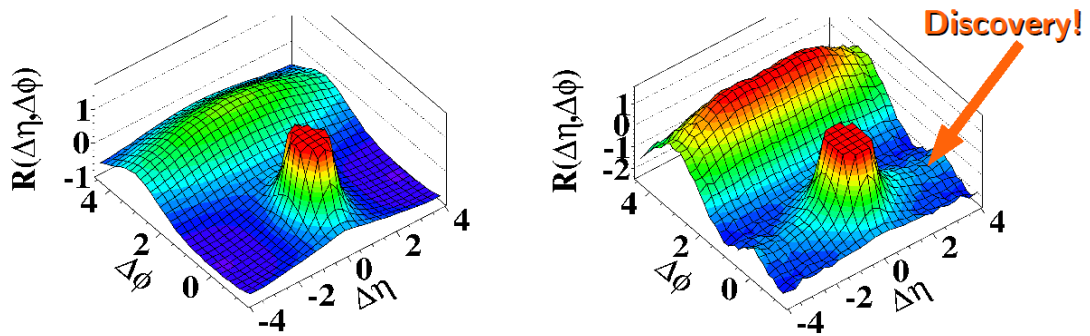


Figure 1: Two particle correlation function from minimum-bias (left) and high-multiplicity (right) events in proton-proton collisions at $\sqrt{s} = 2.76$ TeV. Data from the CMS collaboration¹.

The ridge in proton-proton and proton-lead collisions is a natural consequence of gluon-saturation and non-linear parton dynamics in the nuclear wave-function *before* the collision occurs. The full structure of the two-particle correlation is explained by two competing QCD diagrams; as long as they are both computed within the CGC-EFT³. The first diagram corresponds to the production of two gluons from a single *ladder* as shown in the right-most Feynman diagram appearing in Fig. 3. This production mechanism creates particles primarily back-to-back (*i.e.* on the away-side for $\Delta\eta \gtrsim 1$) and does not generate any near-side collimation. A second class of diagrams, herein called “Glasma Graphs”, where two gluons are produced from different ladders, is responsible for the near-side collimation identified with the ridge. The two-



Figure 2: The ridge in La Thuile on March 14th 2013.

particle correlation generated by the Glasma graphs is symmetric with respect to $\Delta\phi = \pi/2$ and therefore produces an equal away-side collimation as well; however, this is hidden underneath the away-side jet and was only recently observed after a careful subtraction of peripheral events.

Saturation dynamics comes into play when determining the relative contribution of these two diagrams towards the two-particle correlation. A power counting exercise demonstrates that the Glasma graph is enhanced by a factor of α_s^{-8} in the presence of saturation, which we associate with central / high-multiplicity collisions. This should be compared to the α_s^{-4} enhancement of the jet-graph in going from min-bias to central collisions.

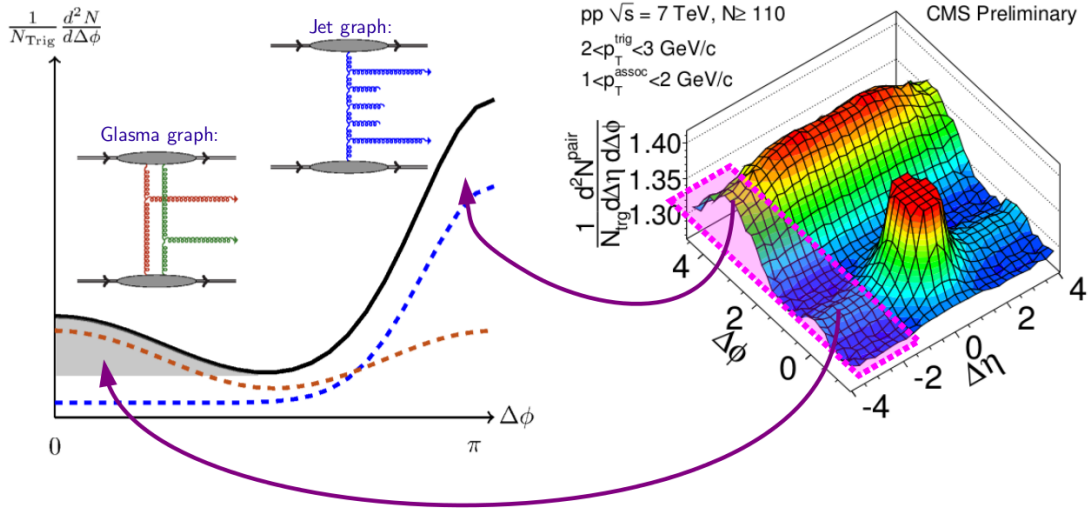


Figure 3: Anatomy of a proton-proton collision. The away-side peak, associated with mini-jet production arises from the jet-graph (two gluons produced from a single ladder) as shown in the right diagram along with its schematic contribution to the per-trigger-yield plotted in blue. The Glasma graph contribution (left diagram) is shown schematically by the orange curve. The shaded gray region (extracted experimentally by the ZYAM procedure) is referred to as the associated yield.

The near-side collimation produced by the Glasma graph can be understood by looking at the schematic form of the double-inclusive cross section

$$d^2\sigma \propto \int_{\mathbf{k}_T} \Phi_A^2(x_1, \mathbf{k}_T) \Phi_B(x_1, \mathbf{p}_T - \mathbf{k}_T) \Phi_B(x_2, \mathbf{q}_T - \mathbf{k}_T) + \dots \quad (1)$$

The full expression used in computations along with all relevant details is presented in ⁴. The function $\Phi(x, \mathbf{k}_T)$ appearing in these expressions is the unintegrated gluon distribution and is obtained by solving the rcBK equation with MV model initial conditions at large x . The Cauchy-Schwarz inequality dictates that the correlation strength at $\Delta\phi = 0$ must be greater than or equal to that at $\Delta\phi = \pi/2$;

$$\int d^2k_{\perp} \Phi_A^2(\mathbf{k}_T) \Phi_B^2(|\mathbf{p}_T - \mathbf{k}_T|) \geq \int d^2k_{\perp} \Phi_A^2(\mathbf{k}_T) \Phi_B(|\mathbf{p}_T - \mathbf{k}_T|) \Phi_B(|\mathbf{q}_T - \mathbf{k}_T|). \quad (2)$$

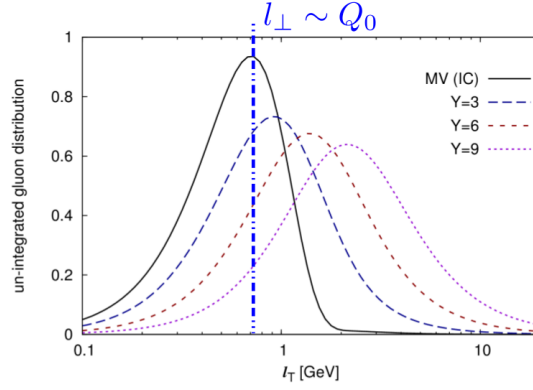


Figure 4: Unintegrated gluon distribution function evolved from the M.V. model initial condition to larger rapidities via the rcBK evolution equation.

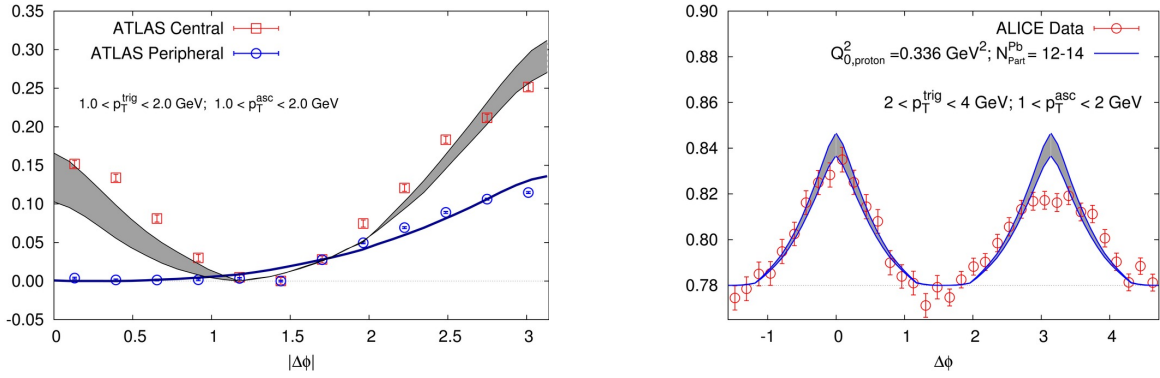


Figure 5: Comparison of calculations within the CGC-EFT framework with recent experiments. The left figure shows the ATLAS⁹ per-trigger-yield as a function of azimuthal separation ($\Delta\phi$) for peripheral events as blue circles and central events as red squares. The solid curves show the theory calculation for these two event classes. For peripheral events only the jet diagram is visible in both the data and theory calculation. The right figure shows data from the ALICE collaboration⁸ where the difference between central and peripheral events allowed for the discovery of the away-side ridge. The gray band shows the contribution from the Glasma graphs.

Furthermore the equality holds if and only if

$$\Phi(|\mathbf{p}_T - \mathbf{k}_T|) \propto \Phi(|\mathbf{q}_T - \mathbf{k}_T|), \quad (3)$$

and therefore, as long as the gluon distribution is a non-trivial function of momentum, there must be a collimation. The strength depends on the detailed structure of the gluon distribution function shown in fig. 4.

The rapid rise of the associated yield (see Fig. 3 for the definition) with centrality for asymmetric collisions can also be understood from equation 1 as well. If we take the unintegrated gluon distribution function as narrowly peaked around the saturation scale Q_A and Q_B of the projectile and target respectively, the associated yield increases quadratically with the larger of the two saturation scales⁵,

$$\text{CY} \propto \frac{\Phi_B(Q_B)}{\Phi_B\left(\sqrt{2p_T^2 + 2Q_A^2 - Q_B^2}\right)} \xrightarrow{Q_B \gg Q_A} 1 + \frac{Q_B^2}{Q_A^2}. \quad (4)$$

A recent work⁶ has compared predictions made within the CGC-EFT to the CMS⁷, ALICE⁸ and ATLAS⁹ experimental data. Two examples of the quality of the theory to data comparison is shown in figure 5. While the CGC-EFT provides a unified description of both p+p and p+Pb collisions at a quantitative level one may still question the role played by final state effects.

While this can only be addressed by detailed modeling there is strong evidence that final state interactions are small and not responsible for the ridge.

A crucial piece of evidence stems from the away-side jet, which remains unmodified from peripheral to central collisions; a fact confirmed a posteriori by the successful subtraction of the peripheral jet from central data by the LHC experimentalists. If final-state rescattering was strong enough to collimate the medium's particles to create the ridge, rescattering should similarly modify the jet. This is indeed observed in heavy-ion collisions but it is not the case in p+p and p+Pb collisions.

A natural question is whether there is a unique final state interpretation of *both* the proton-proton and proton-lead ridge? The differences in systematics between these two systems is naturally understood within the CGC framework. Whether there is a consistent final-state model is far from clear. It seems extremely difficult for a final-state interpretation to account for an associated yield four times larger in p+Pb than in p+p at the *same* multiplicity, considering our expectation that the overlap areas in the two systems are approximately the same.

There is compelling evidence that the ridge in proton-proton and proton-lead collisions is a consequence of gluon saturation and non-linear gluon dynamics. This remarkable discovery of a novel collimation between two particles flying in opposite directions in ultra-rare high multiplicity events is probing rare quantum fluctuations within the proton and nucleus at the smallest length scales experimentally possible.

Acknowledgments

Supported by the US Department of Energy under Contract No. DE-FG02-03ER41260.

References

1. V. Khachatryan *et al.* [CMS Collaboration], JHEP **1009**, 091 (2010) [arXiv:1009.4122 [hep-ex]].
2. K. Dusling and R. Venugopalan, Phys. Rev. Lett. **108**, 262001 (2012) [arXiv:1201.2658 [hep-ph]].
3. F. Gelis, E. Iancu, J. Jalilian-Marian and R. Venugopalan, Ann. Rev. Nucl. Part. Sci. **60**, 463 (2010) [arXiv:1002.0333 [hep-ph]].
4. K. Dusling and R. Venugopalan, Phys. Rev. D **87**, 051502 (2012) [arXiv:1210.3890 [hep-ph]].
5. K. Dusling and R. Venugopalan, Phys. Rev. D **87**, 054014 (2012) [arXiv:1211.3701 [hep-ph]].
6. K. Dusling and R. Venugopalan, Phys. Rev. D to appear [arXiv:1302.7018 [hep-ph]].
7. S. Chatrchyan *et al.* [CMS Collaboration], Phys. Lett. B **718**, 795 (2013) [arXiv:1210.5482 [nucl-ex]].
8. B. Abelev *et al.* [ALICE Collaboration], arXiv:1212.2001 [nucl-ex].
9. G. Aad *et al.* [ATLAS Collaboration], arXiv:1212.5198 [hep-ex].